Journal Name

COMMUNICATION

Dynamic covalent assembly and disassembly of nanoparticle aggregates

Received 00th January 20xx,
Accepted 00th January 20xx

DOI: 10.1039/x0xx00000x

www.rsc.org/

Stefan Borsley and Euan R. Kay*

The quantitative assembly and disassembly of a new type of dynamic covalent nanoparticle (NP) building block is reported. In situ spectroscopic characterization reveals constitutionally adaptive NP-bound monolayers of boronate esters. Ditopic linker molecules are used to produce covalently connected AuNP assemblies, displaying open dendritic morphologies, and which, despite being linked by covalent bonds, can be fully disassembled on application of an appropriate chemical stimulus.

Reliable methods for predictable and stimuli-responsive control over nanoparticle (NP) assembly will lead to switchable functional materials exploiting the emergent and collective properties that arise when several NPs are brought together.[1] NP-bound molecular ligands that engage in specific intermolecular interactions offer the opportunity to direct assembly and control structural parameters,[2] independent of the nature of the underlying NP. Particularly successful strategies have exploited noncovalent interactions between NP-bound oligonucleotides,[3] polypeptides,[4] or protein receptor–substrate binding.[5] However, these methods are restricted by the inherent structural features and stability properties of the biomolecule components. Abiotic linkers can access the full gamut of synthetic molecular architectures for optimizing structure, function and properties. Examples involving noncovalent interactions including hydrogen bonds,[6] dipole–dipole interactions,[7] π–π interactions,[8] halogen bonds,[9] metal coordination,[10] and hydrophobic interactions,[11] have yielded some remarkable advances. However, complex molecular designs are often required in order to achieve adequate stability using inherently weak interactions, while reversible or stimuli-responsive control over NP aggregation remains challenging.[6b,7–8,12] A general and simple approach to rival the biomolecular systems has yet to emerge.

We recently introduced dynamic covalent modification of NP-bound monolayers,[13] a powerful strategy that combines the error-correcting and reversible features of equilibrium processes with the stability and structural diversity of covalent chemistry.[14] Using AuNPs bearing a hydrazone-terminated surface monolayer, dynamic covalent exchange was harnessed to reversibly switch the monolayer molecular structure between multiple kinetically stable states, producing concomitant changes in NP physicochemical properties.[13] Independently, Otto and co-workers have demonstrated that a dynamic covalent library of kinetically labile and thermodynamically unstable AuNP-bound imines responds to the introduction of DNA templates.[15]

While hydrazone exchange tends to occur on a timescale of minutes to hours, boronic acids react with various dihydroxy compounds to yield boronate esters extremely rapidly in the presence of Lewis bases.[14] Hydrazones and boronate esters are therefore chemically orthogonal dynamic covalent functionalities displaying an attractive contrast in kinetic characteristics. Under pseudo-irreversible conditions, condensation or hydrolysis of sparsely arranged NP-associated boronate esters has previously been proposed as the operating mechanism in a number of systems for enriching polyhydroxylated biomolecules,[16] or releasing cargoes from mesoporous materials.[17] Here, we create single-component monolayers of structurally simple boronic acids on AuNPs, and establish in situ molecular-level characterization of NP-bound constitutional adaptation through thermodynamically controlled boronate ester exchange. These densely functionalized dynamic covalent NPs represent a new category of nanomaterial building block, which can be combined in a modular fashion with molecular linkers to create covalently connected, but stimuli-responsive assemblies.

Gold nanoparticles AuNP-**1** (Fig. 1a), stabilized by a single-component boronic acid terminated surface monolayer, were

EaStCHEM School of Chemistry, University of St Andrews, North Haugh, St Andrews, KY16 9ST, UK. E-mail: ek28@st-andrews.ac.uk

† Electronic Supplementary Information (ESI) available: Synthetic procedures and characterization data for all compounds and AuNPs; experimental procedures; additional TEM images; details of control assembly experiments. See DOI: 10.1039/x0xx00000x

This work was supported by the EPSRC (EP/K016342/1 and EP/J500549/1), the University of St Andrews and by a Royal Society of Edinburgh/Scottish Government Fellowship (E.R.K.). We thank Dr Lorna Eades for ICP-OES measurements, and are grateful to Mr Ross Blackley for assistance with TEM imaging. Mass spectrometry was carried out at the EPSRC UK National Mass Spectrometry Facility (NMSF) at Swansea University. We thank Professor Douglas Philp for helpful discussions.

prepared in one step by reduction of $AuPPh_3Cl$ in the presence of disulfide $\mathbf{1}_2$, yielding relatively monodisperse samples with mean diameter ≈ 3.4 nm (Fig. S1, ESI†). Following removal of unbound molecular species by several cycles of precipitation and washing, stable colloidal suspensions corresponding to high concentrations of NP-bound ligand **1** could be achieved in MeOH. This enabled direct molecular-level characterization of the monolayer by NMR spectroscopy. Analysis by ^{1}H NMR in situ (Fig. S2, ESI†), and following oxidative ligand stripping (Fig. S3, ESI†), confirmed a homogeneous monolayer of boronic acids **1** and the absence of any other molecular species. Elemental analysis was also consistent with a uniform monolayer of **1** (Au:S:B = 7.3:1.0:0.97; ca. 170 ligands per NP, Table S1, ESI†).

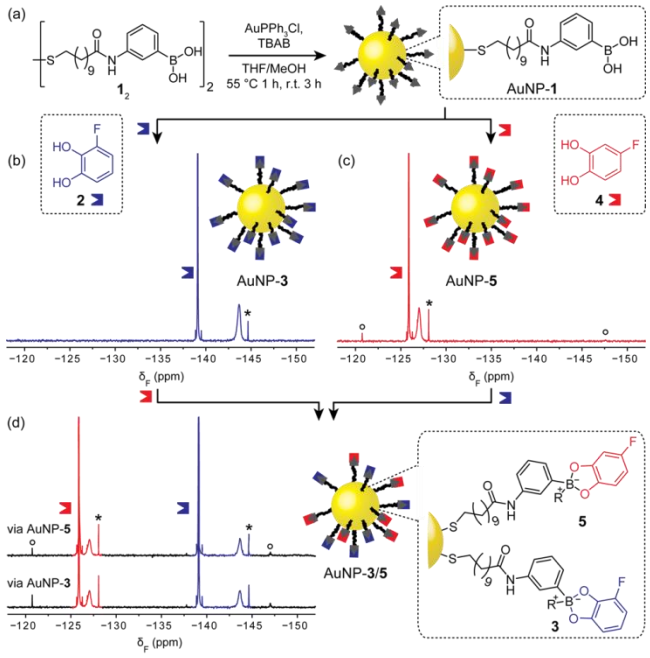

Fig. 1 NP-Bound boronate ester formation and dynamic covalent exchange. (a) Preparation of AuNP-**1**. TBAB = borane *tert*-butylamine. (b,c,d) Partial $^{19}F\{^1H\}$ NMR spectra (10:1 CD_3OD/CD_2Cl_2, 470.5 MHz, 298 K) indicating surface-saturated NP-bound boronate ester formation in the presence of: (b) catechol **2**; (c) catechol **4**. (d) Identical mixed monolayer compositions of NP-bound boronate esters **3** and **5** prepared from either surface saturated AuNP-**3** (bottom trace) or AuNP-**5** (top trace). Initial concentrations: (b) $[\text{AuNP-}\mathbf{1}]_0$ = 9.0 mM, $[\mathbf{2}]_0$ = 26 mM, $[\mathbf{4}]_0$ = 0.0 mM; (c) $[\text{AuNP-}\mathbf{1}]_0$ = 9.0 mM, $[\mathbf{2}]_0$ = 0.0 mM, $[\mathbf{4}]_0$ = 26 mM; (d) $[\text{AuNP-}\mathbf{1}]_0$ = 9.0 mM, $[\mathbf{2}]_0$ = 26 mM, $[\mathbf{4}]_0$ = 26 mM; all samples: [*N*-methylmorpholine] = 900 mM.[§] Signals marked * correspond to desorbed ligand, which appears slowly in the presence of base; signals marked ° arise from oxidative decomposition of **4**. The sum of all impurities amounts to < 4 % of total fluorine-containing species. R = *N*-methylmorpholinium.

A suspension of AuNP-**1** was prepared in CD_3OD/CD_2Cl_2 (10:1) at a concentration of 9.0 mM in terms of **1**. When 3-fluorocatechol (**2**) was added to this sample, a single, sharp signal was observed in the $^{19}F\{^1H\}$ NMR spectrum, indicating no interaction between the catechol and the NP-bound boronic acids. On addition of a Lewis base such as *N*-methylmorpholine,[§] a broad signal immediately appeared upfield of the sharp catechol resonance (Fig. 1b), at a chemical shift closely matching that of model molecular aryl boronate esters formed from **2** (Fig. S12, ESI†). The significant signal broadening (fwhm ≈ 132 Hz) is characteristic of NP-bound species,[18] thus confirming the presence of NP-bound boronate ester **3** and free catechol **2** in slow exchange on the NMR timescale. The concentration of **3** could readily be determined by integration of the broad signal relative to an internal standard, and was observed to increase with increasing concentration of **2** until saturation was reached after addition of ca. 15 mM **2** (1.7 equivalents with respect to **1**, Fig. S8, ESI†). At this point, the surface saturation concentration of NP-bound boronate esters was 7.9 mM, corresponding to 89% of all NP-bound **1**. The sub-stoichiometric surface functionalization is likely a result of steric and/or electrostatic repulsion between monolayer-bound boronate esters, and is consistent with a simple geometric model of the space available at the terminus of each NP-bound ligand (ESI† Section 4.3).

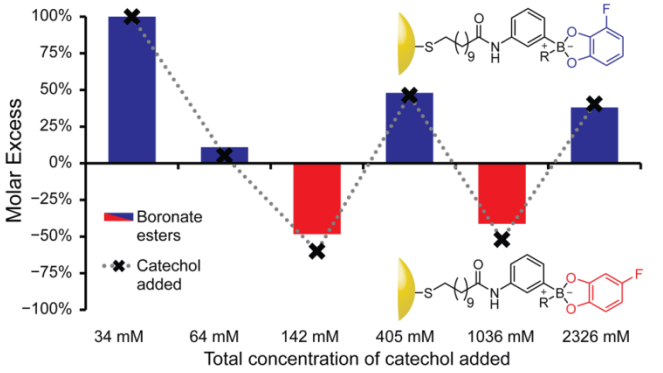

Fig. 2 Constitutional adaptation for NP-bound mixed monolayers of boronate esters AuNP-**3/5** (R = *N*-methylmorpholinium). Monolayer composition repeatedly and rapidly adjusts in response to changing the molar excess of catechols **2** and **4** over several cycles, irrespective of the total concentration of exogenously added catechol.

On adding to surface-saturated AuNP-**3** an equimolar quantity (with respect to total added **2**) of 4-fluorocatechol (**4**), a second pair of broad and sharp peaks is observed in the ^{19}F NMR spectrum, corresponding to NP-bound boronate ester **5** and unbound **4** (Fig. 1d, bottom trace). The monolayer of boronate ester **3** had been successfully converted into a mixed monolayer of esters **3** and **5**. Similarly, starting with the addition of catechol **4** to AuNP-**1**, a monolayer of boronate ester **5** was obtained (Fig. 1c, surface saturation concentration 8.3 mM, 93%). Subsequent dynamic covalent exchange with catechol **2** again gave a mixed monolayer of **3** and **5** (Fig. 1d, top trace). Crucially, the compositions of the two AuNP-**3/5** mixed monolayers produced via each pathway were identical (Fig. 1d, both traces [**3**] = 3.8 mM; [**5**] = 3.7 mM), evincing a reconfigurable dynamic equilibrium with composition that is independent of the preparation route.

The population of NP-bound boronate esters showed adaptive behaviour on sequential addition of catechols **2** and **4** over several cycles, producing mixed monolayer compositions that reflect the molar excess of catechol present, irrespective of the overall concentration (Fig. 2). After each addition, equilibrium was achieved within the time required to record an NMR

spectrum. The rapid dynamic covalent exchange of boronate esters proceeds under thermodynamic control even within the crowded environment of a NP-bound monolayer.

We reasoned that the dynamic exchange of covalently linked NP-bound functionality offers a new strategy for preparing NP self-assemblies under thermodynamic control, but connected by covalent bonds (Fig. 3). Consequently, bifunctional catechol linker **6** (15 equivalents relative to **1**) was added to a suspension of AuNP-**1** (0.1 mg mL^{-1} in $MeOH/CH_2Cl_2$/*N*-methylmorpholine 90:9:1 v/v, corresponding to ca. 40 μM in terms of **1**). Initially, no change was observed either by eye or by UV-Vis analysis. However, after a total of 5 days, complete NP precipitation had occurred.[§§] On TEM imaging of the precipitates (Fig. 4b, S20, S21, ESI†), no isolated NPs could be observed; the entire sample had been incorporated into extended assemblies. Areas where the assemblies lie just a few NP thick allowed the morphology to be visualized as an open network of interconnected strands with consistent width. The same structure was also evident where overlapping strands produced 3D aggregates, and was repeated across several images, and for replicate samples (Fig. S20, ESI†). Assembly of low density NP structures of this nature, consistent with a diffusion-limited aggregation process,[19] can be challenging to control,[7b,10,20] and to our knowledge has never before been reported for NP assemblies linked by covalent bonds.

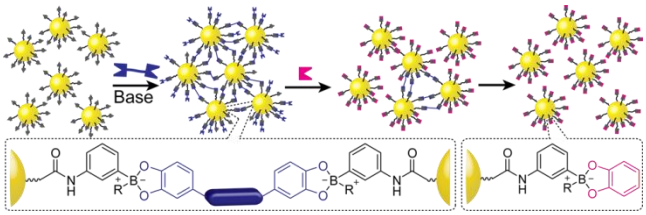

Fig. 3 Schematic representation of boronate ester-driven dynamic covalent nanoparticle assembly and disassembly on sequential addition of a bifunctional linker and a monofunctional capping unit. R = *N*-methylmorpholinium.

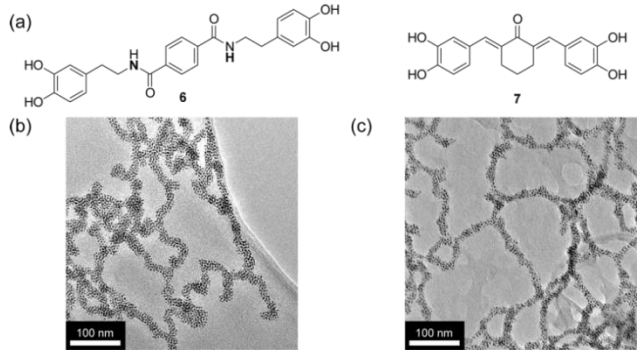

Fig. 4 (a) Chemical structures of bifunctional catechol linkers **6** and **7**. (b,c) Representative TEM images of the assemblies formed on treating AuNP-**1** with linker **6** or **7**, respectively. For several more images of each assembly, see ESI†.

The precipitation of extended NP aggregates represents a kinetic trap state during the self-assembly process. Nonetheless, these solid-state aggregates are linked by reversible covalent bonds, and should correspondingly exhibit responsive behaviour. Monofunctional 1,2-dihydroxybenzene (140 mM) was added to a fully precipitated sample assembled from AuNP-**1** and linker **6**. The sample was occasionally agitated in an ultrasonic bath, leading to gradual NP redispersion. After a period of 35 days, solid material could no longer be observed by eye, and TEM imaging revealed a mixture individual NPs, along with small, spherical NP clusters of up to 50 nm in diameter (Fig. 5c, S26, ESI†). After a further 7 days, microscopic analysis revealed a fully disaggregated state, which at the nanoscale was completely indistinguishable from the starting point (Fig. 5d, S27, ESI†). Despite the heterogeneous nature of the disassembly process (and with only sporadic agitation), it is possible to switch between solid-state, covalently linked extended NP networks, and fully dispersed, colloidally stable individual NPs driven by dynamic covalent exchange reactions.

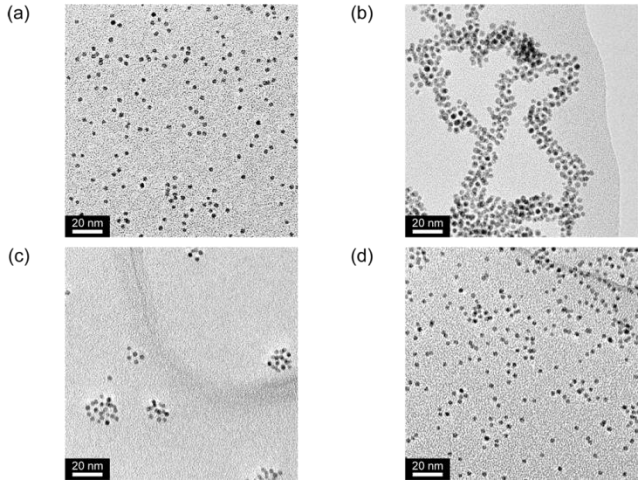

Fig. 5 Assembly and disassembly of covalently linked NP aggregates. TEM images of: (a) AuNP-**1**; (b) assembly formed on treating AuNP-**1** with bifunctional linker **6**; (c) colloidally stable discrete assemblies observed after treating the fully precipitated aggregate in (b) with 1,2-dihydrozybenzene for 35 days; (d) fully disassembled AuNPs formed from (b) after a total of 42 days in the presence of 1,2-dihydroxybenzene. For several more images of each stage, see ESI†.

Colloidal suspensions of AuNP-**1**, in the absence of either linker **6** or a Lewis base, are entirely stable for at least 20 days (monitored by UV-Vis), and show no change by eye over much longer time periods (> 1 year), indicating that NP assembly and precipitation is a direct consequence of covalent boronate ester links. Furthermore, NPs of a similar size, bearing a structurally related monolayer that lacks the boronic acid functionality, showed no signs of aggregation in the presence of **6** and *N*-methylmorpholine, ruling out nonspecific interactions involving the linker, or its deprotonated forms (ESI† Section 6.2).

Linking NPs through specific molecular interactions introduces the possibility of tuning the assembly process – and therefore aggregate morphology – through structural changes to the linker. It might be expected that linker **6** can engage in bivalent binding of both catechols to the same AuNP. Rigid bis-catechol **7** should be less likely to adopt such an arrangement, and under otherwise identical conditions produced aggregates that exhibit a significantly more open network, characterized by chains of fewer NPs in width and with longer average distance between the branch points (Fig. 4c, S22, ESI†). Model

compound studies indicate that **7** forms more stable boronate esters than **6**, and we hypothesize that this is the key difference affecting aggregate morphology. The boronate ester dissociation constant controls the extent to which aggregation follows diffusion-limited or reaction-limited kinetics, and this in-turn determines the final aggregate morphology.[19] Investigations are currently under way to quantify these interactions within the NP-bound monolayer, and link molecular-level understanding of the dynamic covalent process to aggregation mechanism and assembly morphology.

In summary, we have developed a new category of dynamic covalent NP building block. In situ spectroscopic characterization has revealed that NP-bound boronate ester exchange on a homogeneous monolayer of boronic acids proceeds rapidly and reversibly; high degrees of surface functionalization can be achieved; and mixed-monolayer compositions are tuneable under thermodynamic control. Dynamic covalent NP-bound monolayers open up a vast new region of chemical space for engineering responsive nanomaterials, unrestricted by the structural or stability constraints of biomolecules or noncovalent systems. They raise the exciting prospect of assembling NPs under error-correcting conditions, yet exploiting stable, structurally unambiguous covalent links. Simple bifunctional linkers produce covalently connected NP assemblies displaying morphologies that are sensitive to molecular structure. Remarkably, despite being linked by covalent bonds, these solid-state aggregates can be disassembled on application of molecular stimuli; the assembly and disassembly processes are quantitative; and both states are indefinitely stable. The ability to characterize NP-bound dynamic covalent processes in situ promises a predictive understanding of how molecular-level details can be manipulated to control assembly morphology. We foresee that this will ultimately lead to a modular and flexible route to responsive NP assemblies where structure on several size-scales is tuned by molecular-level features, and can be remotely reconfigured by applying chemical or physical stimuli.

Notes and references

§ A high concentration of base (900 mM, 100 equivalents with respect to **1**) was used to ensure quantitative consistency across all NMR experiments. However, the same behaviour is observed at much lower base concentrations (see ESI† Section 4).

§§ At no stage was a shift in the NP plasmon resonance observed. This is not unexpected for small NPs ($d \approx 3.4$ nm) connected by molecular linkers that restrict interparticle distances to values significantly greater than d. The aggregation process could still be followed by the decrease in UV-Vis extinction resulting from NP precipitation from colloidal suspension (see ESI† Section 5.1).

1 (a) C. L. Choi and A. P. Alivisatos, *Annu. Rev. Phys. Chem.*, 2010, **61**, 369; (b) Z. H. Nie, A. Petukhova and E. Kumacheva, *Nature Nanotech.*, 2010, **5**, 15; (c) L. Xu, W. Ma, L. Wang, C. Xu, H. Kuang and N. A. Kotov, *Chem. Soc. Rev.*, 2013, **42**, 3114.

2 (a) R. A. Sperling and W. J. Parak, *Philos. Trans. R. Soc., A*, 2010, **368**, 1333; (b) W. Edwards and E. R. Kay, *ChemNanoMat*, 2016, **2**, 87.

3 (a) C. A. Mirkin, R. L. Letsinger, R. C. Mucic and J. J. Storhoff, *Nature*, 1996, **382**, 607; (b) A. P. Alivisatos, K. P. Johnsson, X. Peng, T. E. Wilson, C. J. Loweth, M. P. Bruchez, Jr. and P. G. Schultz, *Nature*, 1996, **382**, 609.

4 (a) M. G. Ryadnov, B. Ceyhan, C. M. Niemeyer and D. N. Woolfson, *J. Am. Chem. Soc.*, 2003, **125**, 9388; (b) M. M. Stevens, N. T. Flynn, C. Wang, D. A. Tirrell and R. Langer, *Adv. Mater.*, 2004, **16**, 915; (c) D. Aili, K. Enander, L. Baltzer and B. Liedberg, *Nano Lett.*, 2008, **8**, 2473; (d) J. Wang, H. Xia, Y. Zhang, H. Lu, R. Kamat, A. V. Dobrynin, J. Cheng and Y. Lin, *J. Am. Chem. Soc.*, 2013, **135**, 11417.

5 (a) W. Shenton, S. A. Davis and S. Mann, *Adv. Mater.*, 1999, **11**, 449; (b) S. Connolly and D. Fitzmaurice, *Adv. Mater.*, 1999, **11**, 1202.

6 (a) A. K. Boal, F. Ilhan, J. E. DeRouchey, T. Thurn-Albrecht, T. P. Russell and V. M. Rotello, *Nature*, 2000, **404**, 746; (b) P. K. Kundu, D. Samanta, R. Leizrowice, B. Margulis, H. Zhao, M. Boerner, T. Udayabhaskararao, D. Manna and R. Klajn, *Nature Chem.*, 2015, **7**, 646.

7 (a) R. Klajn, K. J. M. Bishop and B. A. Grzybowski, *Proc. Natl. Acad. Sci., U.S.A.*, 2007, **104**, 10305; (b) R. W. Taylor, T. C. Lee, O. A. Scherman, R. Esteban, J. Aizpurua, F. M. Huang, J. J. Baumberg and S. Mahajan, *ACS Nano*, 2011, **5**, 3878.

8 R. Klajn, M. A. Olson, P. J. Wesson, L. Fang, A. Coskun, A. Trabolsi, S. Soh, J. F. Stoddart and B. A. Grzybowski, *Nature Chem.*, 2009, **1**, 733.

9 T. Shirman, T. Arad and M. E. van der Boom, *Angew. Chem. Int. Ed.*, 2010, **49**, 926.

10 (a) V. Lesnyak, A. Wolf, A. Dubavik, L. Borchardt, S. V. Voitekhovich, N. Gaponik, S. Kaskel and A. Eychmueller, *J. Am. Chem. Soc.*, 2011, **133**, 13413; (b) A. Singh, B. A. Lindquist, G. K. Ong, R. B. Jadrich, A. Singh, H. Ha, C. J. Ellison, T. M. Truskett and D. J. Milliron, *Angew. Chem. Int. Ed.*, 2015, **54**, 14840.

11 (a) J. Liu, S. Mendoza, E. Román, M. J. Lynn, R. L. Xu and A. E. Kaifer, *J. Am. Chem. Soc.*, 1999, **121**, 4304; (b) J. Zhang, R. J. Coulston, S. T. Jones, J. Geng, O. A. Scherman and C. Abell, *Science*, 2012, **335**, 690.

12 (a) A. Manna, P.-L. Chen, H. Akiyama, T.-X. Wei, K. Tamada and W. Knoll, *Chem. Mater.*, 2003, **15**, 20; (b) R. Klajn, P. J. Wesson, K. J. M. Bishop and B. A. Grzybowski, *Angew. Chem. Int. Ed.*, 2009, **48**, 7035; (c) Y. H. Wei, S. B. Han, J. Kim, S. L. Soh and B. A. Grzybowski, *J. Am. Chem. Soc.*, 2010, **132**, 11018; (d) S. Das, P. Ranjan, P. S. Maiti, G. Singh, G. Leitus and R. Klajn, *Adv. Mater.*, 2013, **25**, 422; (e) A. Koehntopp, A. Dabrowski, M. Malicki and F. Temps, *Chem. Commun.*, 2014, **50**, 10105; (f) J.-W. Lee and R. Klajn, *Chem. Commun.*, 2015, **51**, 2036; (g) D. Manna, T. Udayabhaskararao, H. Zhao and R. Klajn, *Angew. Chem. Int. Ed.*, 2015, **54**, 12394.

13 F. della Sala and E. R. Kay, *Angew. Chem. Int. Ed.*, 2015, **54**, 4187.

14 (a) S. J. Rowan, S. J. Cantrill, G. R. L. Cousins, J. K. M. Sanders and J. F. Stoddart, *Angew. Chem. Int. Ed.*, 2002, **41**, 898; (b) Y. Jin, C. Yu, R. J. Denman and W. Zhang, *Chem. Soc. Rev.*, 2013, **42**, 6634.

15 P. Nowak, V. Saggiomo, F. Salehian, M. Colomb-Delsuc, Y. Han and S. Otto, *Angew. Chem. Int. Ed.*, 2015, **54**, 4192.

16 (a) W. Zhou, N. Yao, G. Yao, C. Deng, X. Zhang and P. Yang, *Chem. Commun.*, 2008, 5577; (b) L. Liang and Z. Liu, *Chem. Commun.*, 2011, **47**, 2255; (c) H. Wang, Z. Bie, C. Lu and Z. Liu, *Chem. Sci.*, 2013, **4**, 4298.

17 (a) E. Aznar, M. Dolores Marcos, R. Martínez-Máñez, F. Sancenón, J. Soto, P. Amorós and C. Guillem, *J. Am. Chem. Soc.*, 2009, **131**, 6833; (b) Y. Zhao, B. G. Trewyn, I. I. Slowing and V. S.-Y. Lin, *J. Am. Chem. Soc.*, 2009, **131**, 8398.

18 Z. Hens and J. C. Martins, *Chem. Mater.*, 2013, **25**, 1211.

19 P. Meakin, *Annu. Rev. Phys. Chem.*, 1988, **39**, 237.

20 D. A. Weitz and M. Oliveria, *Phys. Rev. Lett.*, 1984, **52**, 1433.

